Katherine A. Gallagher,[1] Amrita Joshi,[1] William F. Carson,[2] Matthew Schaller,[2]
Ronald Allen,[2] Sumanta Mukerjee,[2] Nico Kittan,[2] Eva L. Feldman,[3] Peter K. Henke,[1]
Cory Hogaboam,[4] Charles F. Burant,[5] and Steven L. Kunkel[2]

Epigenetic Changes in Bone Marrow Progenitor Cells Influence the Inflammatory Phenotype and Alter Wound Healing in Type 2 Diabetes

COMPLICATIONS

Classically activated (M1) macrophages are known to play a role in the development of chronic inflammation associated with impaired wound healing in type 2 diabetes (T2D); however, the mechanism responsible for the dominant proinflammatory (M1) macrophage phenotype in T2D wounds is unknown. Since epigenetic enzymes can direct macrophage phenotypes, we assessed the role of histone methylation in bone marrow (BM) stem/progenitor cells in the programming of macrophages toward a proinflammatory phenotype. We have found that a repressive histone methylation mark, H3K27me3, is decreased at the promoter of the *IL-12* gene in BM progenitors and this epigenetic signature is passed down to wound macrophages in a murine model of glucose intolerance (diet-induced obese). These epigenetically "preprogrammed" macrophages result in poised macrophages in peripheral tissue and negatively impact wound repair. We found that in diabetic conditions the H3K27 demethylase Jmjd3 drives *IL-12* production in macrophages and that *IL-12* production can be modulated by inhibiting Jmjd3. Using human T2D tissue and murine models, we have identified a previously unrecognized mechanism by which macrophages are programmed toward a proinflammatory phenotype, establishing a pattern of unrestrained inflammation associated with nonhealing wounds. Hence, histone demethylase inhibitor–based therapy may represent a novel treatment option for diabetic wounds.

According to the Centers for Disease Control and Prevention, 9.6% of the population over 20 years of age suffers from diabetes, with an estimated economic cost of 200 billion dollars, with a third of the burden due to peripheral wounds (1). Impaired cutaneous wound healing is the most prevalent cause of hospitalization in patients with type 2 diabetes (T2D) and the most common cause of lower extremity amputation in the U.S. Wound repair is a complex process that involves the local tissue environment, resident cells that proliferate and migrate, and systemic mobilization and differentiation of bone marrow (BM)–derived cells (2,3). In normal wound healing, myeloid cells are mobilized from the BM into the circulation and migrate into the peripheral tissues where they differentiate into macrophages, a key immune cell that drives wound inflammation (4,5). Classically activated macrophages (M1) express a defined set of proinflammatory mediators, in contrast to alternatively activated macrophages (M2), which perform a more regulatory role (6,7). The proinflammatory macrophages promote an inflammatory immune response through the production of cytokines, including interleukin-12 (IL-12) (8,9). Under normal wound healing conditions, macrophages initially secrete proinflammatory mediators (i.e., IL-12) performing antimicrobial functions (10,11). This is followed by conversion to an anti-inflammatory macrophage phenotype (M2) promoting tissue repair (12). Although transient inflammation is an integral part of successful wound healing, it is necessary that the inflammatory phase resolves in a timely fashion in order to allow the healing cascade to progress. Clinically in T2D, this macrophage functional/phenotypic switch does not readily occur and

[1]Department of Surgery, University of Michigan, Ann Arbor, MI
[2]Department of Pathology, University of Michigan, Ann Arbor, MI
[3]Department of Neurology, University of Michigan, Ann Arbor, MI
[4]Department of Medicine, Cedars-Sinai, Los Angeles, CA
[5]Department of Medicine, University of Michigan, Ann Arbor, MI

Corresponding author: Katherine A. Gallagher, kgallag@med.umich.edu.

the macrophages remain predominantly in a proinflammatory, M1-activation state and chronic inflammation ensues (11,13,14).

Evidence suggests that epigenetic regulation (e.g., DNA methylation, histone modification) of gene expression plays a key role in influencing immune cell phenotypes (15). Epigenetic modifications have been documented in inflammation and have been shown to regulate downstream immune mediator expression in monocyte-derived macrophages (16,17). Although the underlying mechanisms are being actively investigated, the notion that gene expression patterns can be maintained over a period of time and are heritable arises because specifically modified histones within nucleosomes can act as templates to initiate identical modifications during replication. Thus, these specific histone modifications can be transferred to more differentiated cells (18).

The contributions of epigenetic-based mechanisms on the regulation of macrophage phenotypes in diabetic wounds are unknown. Although histone methylation changes have been shown to influence macrophage phenotypes, the effects in T2D or in wounds have not been addressed. Histone methylation is important as it plays a key role in maintaining active or suppressed gene expression depending on the methylation site. Methylation of lysine 27 (K27) of histone 3 (H3) keeps the chromatin in a confirmation such that the promoter for specific genes is unavailable for transcription and thus genes are silenced (17,19,20). In contrast to this, methylation of lysine 4 on H3 opens up the chromatin and allows for gene expression (16). In this study, we hypothesized that histone methylation changes are induced in BM cells and set a "metabolic memory" phenomenon, resulting in peripheral macrophages that are predisposed toward a proinflammatory phenotype in the setting of the glucose intolerance. We further hypothesized that this macrophage phenotype contributes to the chronic inflammation observed in T2D peripheral wounds. These results validate our hypothesis and show for the first time that histone methylation influences macrophages toward a proinflammatory response in diabetic wounds and plays an essential role in the initiation and maintenance of chronic wound inflammation.

RESEARCH DESIGN AND METHODS

Mice
Mice were maintained in the University of Michigan pathogen-free animal facility, and all protocols were approved by and in accordance with the guidelines established by the Institutional Animal Care and Use Committee (UCUCA). Male C57BL/6 mice maintained on a normal chow diet (ND) (13.5% kcal fat; LabDiet) or high-fat diet (HFD) (60% kcal fat; Research Diets, Inc.) were purchased at 20 weeks from The Jackson Laboratory (Bar Harbor, ME). Animals underwent all procedures at 22–26 weeks of age. Body weights and insulin levels were determined prior to experimentation. Wounds were

induced on the back using a 4-mm punch biopsy. Full-thickness skin was removed, exposing the underlying muscle. Two wounds per mouse were made in such a manner. A 6-mm punch biopsy was used to harvest wounds.

Assessment of Wound Healing
Initial wound surface area was recorded and digital photographs were obtained daily using an Olympus digital camera. Photographs contained an internal scale to allow for standard measurement calibration. Wound area was quantified using ImageJ software (National Institutes of Health, Bethesda, MD) and was expressed as the percentage of original wound size over time.

Flow Cytometry
Human or mouse cells were harvested and Fc receptors of cells were blocked with anti-CD16/32 (BioLegend) or human IgG (Sigma-Aldrich) for 10 min followed by staining of cells for 15 min at room temperature. For intracellular staining, cells were fixed in 2% formaldehyde and then permeabilized using the Perm/Wash buffer kit (BD Biosciences) followed by antibody incubation. Monoclonal antibodies used for flow cytometry include the following: anti–c-Kit, anti-Sca1, anti-CD48, anti-CD150, anti-Flt3 ligand, anti-CD3, anti-TER119, anti–Gr-1, and anti-B220 (BioLegend) for mouse studies and anti-CD68 (BioLegend), anti-CD163 (Biolegend), and anti-206 (eBioscience) for human studies. Rabbit antitrimethylated H3K4 (Abcam) and antitrimethylated H3K27 (Millipore) were used to detect histone marks, followed by secondary stain with FITC-AffiniPure goat anti-rabbit IgG (Jackson ImmunoResearch). All populations were routinely back gated to verify purity and gating. Samples were analyzed on an LSR II (BD Biosciences). One million viable cells were analyzed. Data were analyzed using FlowJo software version 9.0 (Tree Star, Inc.) and compiled using Prism (GraphPad Software).

Cell Culture and Cytokine Analysis
BM cells were collected by flushing mouse femurs and tibias with RPMI. BM-derived macrophages (BMDMs) were cultured as previously detailed (21). On day 6, the cells were replated, and after resting for 24 h, they were incubated with or without IFN-γ (100 ng/mL) and LPS (100 ng/mL) for 6–48 h. GSK-J4 (R&D Systems) was used as previously described (20).

Microscopy
Wounds were harvested, paraffin embedded, and examined using HRP-DAB staining kit (R&D Systems). The slides were stained with anti-CD86 (BD Biosciences) overnight at 4°C followed by secondary antibody stain for 1 h at room temperature. Cells were observed under an Olympus microscope, and images were captured using cellSens software (Center Valley, PA).

Chromatin Immunoprecipitation Assay
The chromatin immunoprecipitation (ChIP) assay was performed as previously described by our group (21,22).

Purified DNA was used in a PCR reaction with oligonucleotide primers to the promoter region of the following genes: IL-12p35 (CAGACTCAGTGTCCACGAT and GCCCAGTGCCCCTTCTAAAGT), Jmjd3 (CAAGCACATTTCACGTACAGATGA and CCACAAAGCCAGAAGGGGTTT), arginase-1 (GTCAGAGAGCAGAAGGCTTTG and GGAAGTCTGAACAATGCCTCA), and mannose receptor (CCGCCCCCATGTGACA and TCCCTTTTAAAGGACTCCTGAA). Primers to detect H3K27me3 along the promoter region of IL-12 are listed in Table 1.

Quantitative RT-PCR

Total RNA extraction was performed using TRIzol per the manufacturer's instructions. Total RNA was reverse transcribed to cDNA with MMLV (Invitrogen, Carlsbad, CA). RT-PCR was performed with 2XTaqman PCR mix using the 7500 Real-Time PCR System. Primers for nitric oxide synthase 2 (NOS2), IL-1β, IL-12, and Jmjd3 were purchased (Applied Biosystems). Gapdh was used as the internal control. All standards and samples were assayed in triplicate. The threshold cycle values were used to plot a standard curve.

ELISA

Mouse IL-12 concentration was measured by the Quantikine mouse IL-12 ELISA kit (R&D Systems) per the manufacturer's protocol. Color intensity was measured at 492 nm. Culture supernatants were obtained at 24 and 48 h. The ELISA kit has a detection limit of 15 pg/mL.

Bioplex

Levels of IL-6, IL-10, IL-12, and tumor necrosis factor-α (TNF-α) were determined using the Luminex/Bioplex assay 200 system (Bio-Rad) per the manufacturer's protocol. The limit of detection for each cytokine was <5 pg/mL. The cytokine levels were normalized to protein present in a cell-free preparation of each sample measured by Bradford Assay (Bio-Rad).

PCR Array Analysis

Wounds from HFD and control mice were digested in collagenase A (Roche, Indianapolis, IN) and passed through 100 μmol/L cell strainer to get a single cell suspension. CD11b$^+$ cells were isolated using a magnetic-associated cell sorting (MACS) column. RNA extracted from CD11b$^+$ cells was concentrated and cleaned using RNAeasyMinElute Cleanup kit (Qiagen, Germantown, MD). RT^2 First Strand kit (Qiagen) was used to reverse transcribe RNA. Gene expression was analyzed using PCR array PAMM-085Z (Qiagen), which includes PCR primers for 84 chromatin-modifying enzymes. Data were analyzed using the PCR Array Data Analysis Web Portal.

Genetic Silencing Using Small Interfering RNA

Lipofectamine RNAiMAX (Invitrogen) was used to transfect murine BMDMs according to the manufacturer's protocol. ON-TARGETplus Jmjd3 small interfering RNA (siRNA) and ON-TARGETplus Non-Targeting pool siRNA were purchased from GE Healthcare. Cells were incubated in serum-free medium (Acell; GE Healthcare) with or without Lipofectamine-siRNA complexes for 48 h, after which the monolayer was washed and stimulated for 24 h using LPS/IFN-γ (100 ng/mL) as described above. Jmdj3 and IL-12 expression was analyzed by RT-PCR. IL-12 production was examined using Bioplex.

Isolation of Human Macrophages From Tissue/BM

A 6-mm punch biopsy of human wound tissue and 30 cc of BM were obtained from T2D and nondiabetic patients (with toe-brachial index >0.3) following amputation under University of Michigan institutional review board–approved protocols. Wound biopsies contained no healthy, nonwounded skin. Patients were male, with a mean age of 63 years. There were no statistical differences between the groups. Comorbid conditions including congestive heart failure, coronary artery disease, chronic renal insufficiency, smoking status, and obesity (BMI >35) were similar between the groups. Immune cell isolations were performed immediately after surgery. Bones were flushed with RPMI supplemented with 10% FBS/penicillin/streptomycin. Tissue was incubated in 0.16% collagenase at 37°C. Cells underwent red blood cell lysis followed by Ficoll separation. Leukocytes were harvested from the buffy coat. Macrophages were cultured from human BM in the presence of 25 ng/mL M-CSF, 2.5 ng/mL GM-CSF, 50 ng/mL SCF, and 20 ng/mL IL-3 (R&D Biosystem) as described previously (23).

Primer #	Site	Forward	Reverse
	Table 1—Oligonucleotide primers on IL-12p35		
1	−116 to −203	AGTTAATTCGAAAGCGCCAC	CTTTCCCAGGACTGTGTCTC
2	−149 to −232	CACACTTTCTTTGCAGGAGC	GATTCCCAGTGGGGTAACAG
3	−432 to −532	CTGATCTCTTCTGTCCAGGC	GGCAACCATCTCCATAACCA
4	−576 to −674	TAGCTCAGAATGCATCCCAC	ATCTCTCTGCAGGAGCCTAA
5	−701 to −850	GTTAGGGACTGTGTCTGGTG	CTTGCCCAGGAGGTTACAAT
6	−1,109 to −1,226	GGACTGCGGAGAAATACTGT	GCTCCATGTTGGAATCTTGC
7	−1,657 to −1,780	CAATGGGCCATATCACCAGA	TTATGGCTGAGGCACAAGTT
8	−2,006 to −2,093	CCTCAACTTCCCCAGTTTCT	TCATAATGTCCAGCAGAGACG
9	−2,821 to −2,890	TTTCTCCTGGACGCTTGAAA	TAATGTCCAGCAGAGACGAC

Statistical Analysis

Data were analyzed using GraphPad Prism software version 6. We expressed the results as means ± SE except when multiple independent groups were used where we expressed results as mean ± SD. The statistical significance of differences between two groups was determined using Student t tests, and differences between more than two groups were evaluated by ANOVA followed by Newman-Keuls post hoc test. P values ≤0.05 were considered significant.

RESULTS

Macrophages Mount a Distinct Proinflammatory Phenotype in Human T2D Wounds

To determine the peripheral macrophage phenotype in human diabetic wound tissue, macrophages were isolated from chronic nonhealing wounds immediately following lower extremity amputation from T2D and nondiabetic patients. Human macrophages are often phenotypically and functionally defined as M1 based on the absence of M2 cell surface markers and the expression of soluble proteins (24). These human wound-derived macrophages (CD68) were analyzed by flow cytometry for M2 surface markers (CD206 and CD163). Macrophages isolated from T2D human wounds showed a significant decrease in M2 scavenger receptors compared with wound macrophages in nondiabetic individuals (Fig. 1A). Functionally, upon stimulation with LPS/IFN-γ, human T2D BMDMs demonstrated exaggerated production of IL-12, a key

proinflammatory cytokine, compared with nondiabetic controls (Fig. 1B).

Delayed Wound Healing in Diet-Induced Obese Mice Is Associated With Increased Proinflammatory Macrophages

We used our established wound healing model in glucose-intolerant, diet-induced obese (DIO) mice and wild-type (WT) controls to examine macrophage phenotypes and their effect on wound T2D healing (25). Data detailing the body weights, glucose tolerance test results, and plasma insulin levels are shown in Supplementary Fig. 1. We hypothesized that our findings in a mouse model of metabolic syndrome and glucose intolerance would mimic our results seen with human T2D macrophages. Wound healing in DIO mice was significantly delayed when compared with controls (Fig. 2A). Both immunohistochemical and flow cytometry analysis of wound tissue from DIO mice demonstrated increased numbers of proinflammatory macrophages compared with WT (Fig. 2B and C). CCR7^{+} was used as a cell surface marker for M1 polarization based on our published data (23). Perhaps more important than the actual cytokine levels in the tissue is the balance between the pro- and anti-inflammatory cytokines in the wound at a given time point. Consistent with this surface marker, functional analysis based on cytokine production as detected by Bioplex revealed increased ratios of IL-12/IL-10 levels in DIO wounds at days 3 and 7 postwounding (Fig. 2D). These findings are consistent with an
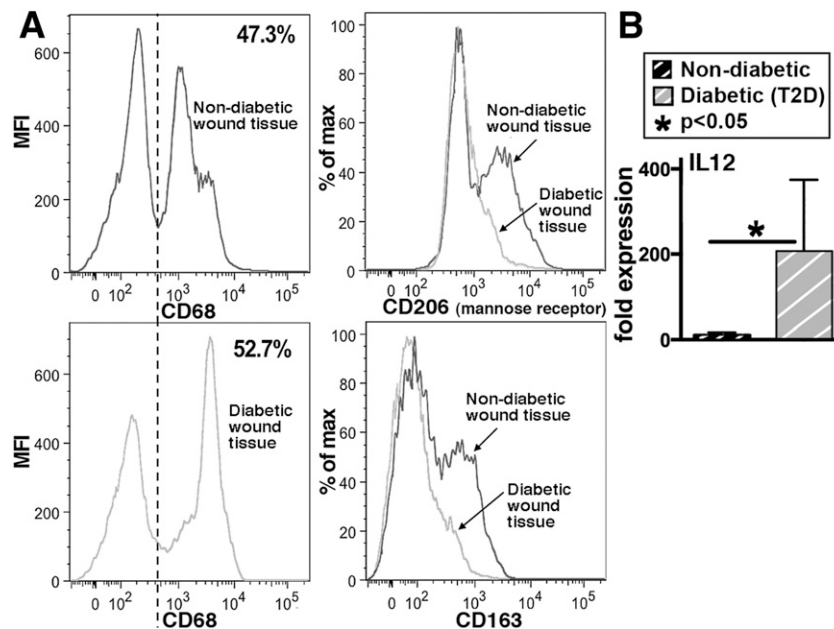
Figure 1—Human wound and BMDMs exhibit decreased anti-inflammatory (M2-like) and increased proinflammatory (M1-like) characteristics in T2D. *A*: Flow cytometry analysis of human macrophages (CD68^{+}) isolated from nonischemic, nondiabetic, and T2D chronic wound tissue. Cells were stained for CD163 and mannose receptor (CD206). Percentage of CD68^{+} cells expressing either CD206 (top right) or CD163 (bottom right) are shown (n = 6). *B*: RT-PCR quantification of *IL-12* (M1 cytokine) expression in human BMDMs 6 h following stimulation with LPS/IFN-γ. BMDMs from T2D patients are compared with BMDMs from nondiabetic patients (n = 6). Data are expressed as mean ± SE. MFI, mean fluorescence intensity.
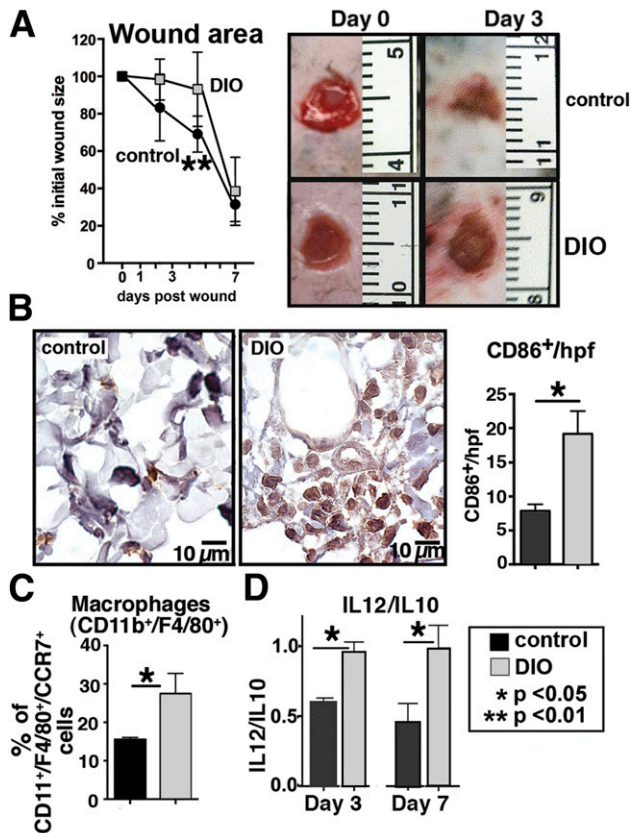
Figure 2—Delayed wound healing in DIO mice is associated with increased proinflammatory macrophages. Punch biopsies (4 mm) were performed on the back of DIO and control mice. Change in wound area was recorded daily using ImageJ software (National Institutes of Health) until complete healing was observed. *A*: Wound healing curves in DIO and control mice (*n* = 10/time point). Data are pooled from three experiments and are expressed as mean ± SD. Representative images of wounds at day 0 and 3 days postwounding are shown. *B*: Immunohistochemical analysis of mononuclear cells (CD86$^+$) in wounds at day 3 (cells/high-powered field [hpf]) in DIO compared with controls (*n* = 6). Representative examples of DIO and control wounds are shown. *C*: Flow cytometry of DIO and control wounds at day 3. Proinflammatory macrophages were defined as CD11b$^+$/F4/80$^+$ cells that coexpressed CCR7 (*n* = 6, experiment replicated once). *D*: Ratio of IL-12 (M1) to IL-10 (M2) cytokine levels in wounds at days 3 and 7 analyzed by Bioplex (*n* = 4, experiment replicated one time). Data are expressed as mean ± SE.

altered balance of macrophages in DIO wounds favoring an increase in proinflammatory macrophages.

BMDMs Are Predisposed Toward an M1, Proinflammatory Phenotype in T2D Murine Model

To examine macrophages derived from the BM in our T2D murine model, BM from DIO and control mice was grown in vitro via standard techniques to culture macrophages. The DIO BMDMs exhibit increased proinflammatory activation as compared with controls as shown by increased inducible NOS2, IL-1β, IL-6, TNF-α, and IL-12 (Fig. 3). This suggests that similar to peripheral tissue macrophages, DIO mice BMDMs display pronounced proinflammatory activity.

DIO BM Stem/Progenitor Cells and Peripheral Macrophages Display Decreased Histone Lysine Trimethylation (H3K27me3) at the Promoter Region of a Key Proinflammatory Macrophage Gene, *IL-12*

Since our data suggest that DIO wound macrophages are poised toward a proinflammatory phenotype, probably set in the BM, we examined BM lin$^-$/c-Kit$^+$ (LK) cells for histone lysine methylation changes that could result in "programmed" changes in peripheral macrophage subsets. We first examined multiple histone methylation marks in murine BM lin$^-$/Sca1$^+$/c-Kit$^+$ (LSK) cells and macrophages (CD11b$^+$/F4/80$^+$). In Fig. 4*A*, both LSK cells and macrophages from DIO mice have significantly decreased levels of H3K27me3, a methylation mark causing transcriptional repression. The H3K27me3 methylation mark maintains the chromatin in a conformation so specific genes are effectively silenced (17).

Since H3K27me3 was decreased in BM LSK and macrophages, we postulated that this repressive mark was decreased on the *IL-12* promoter, a proinflammatory cytokine primarily produced by macrophages that we found was increased in both human T2D and murine DIO wounds. Importantly, IL-12 has been shown to be an important cytokine produced in excess by T2D macrophages in adipose tissue (26). Using ChIP assays, we found H3K27me3 was significantly decreased on the *IL-12* gene promoter in DIO BM stem/progenitor cells (LK), peripheral wound macrophages (CD11b$^+$), and EWAT macrophages (CD11b$^+$) compared with controls (Fig. 4*B–D*). We further examined multiple sites along the *IL-12* promoter in BMDMs and found that DIO mice have decreased H3K27me3 methylation at multiple sites along the *IL-12* promoter (Fig. 4*E*). This likely corresponds to the increased IL-12 protein expression seen in the DIO macrophages. These changes in histone methylation on the *IL-12* promoter detected by ChIP in BM LK cells, BMDMs, and CD11b$^+$ cells from wounds were also seen in *db/db* mice, a genetic model of T2D (Supplementary Fig. 2*A–D*). ChIP analysis of the promoter of two M2-associated genes demonstrated no differences in H3K27 methylation in DIO BMDMs compared with controls (Supplementary Fig. 3*A* and *B*). These data suggest that histone methylation changes may affect gene expression in multiple T2D models and that IL-12 gene expression may be altered by H3K27me3 methylation.
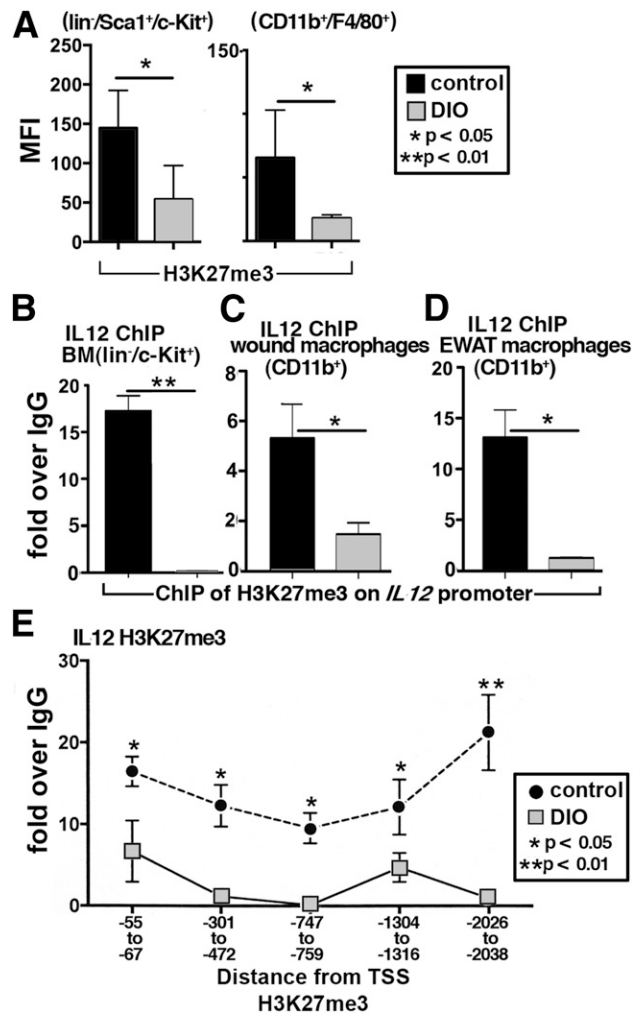
The JumanjiC Domain–Containing Protein, Jmjd3, Is Responsible for the Decrease in the H3K27me3 Repressive Methylation Mark Seen in BM LK Cells and BMDMs

The JumanjiC (JmjC) family of histone demethylases provides essential components of transcriptional chromatin complexes and acts to demethylate lysine residues on histones in a methylation-state and sequence-specific fashion. Jmjd3 specifically removes methyl groups from H3K27me3, effectively eliminating the repressive function of H3K27me3, and thus allows for increased gene expression (27,28). Previous studies from our laboratory and others have shown that Jmjd3 plays a role in
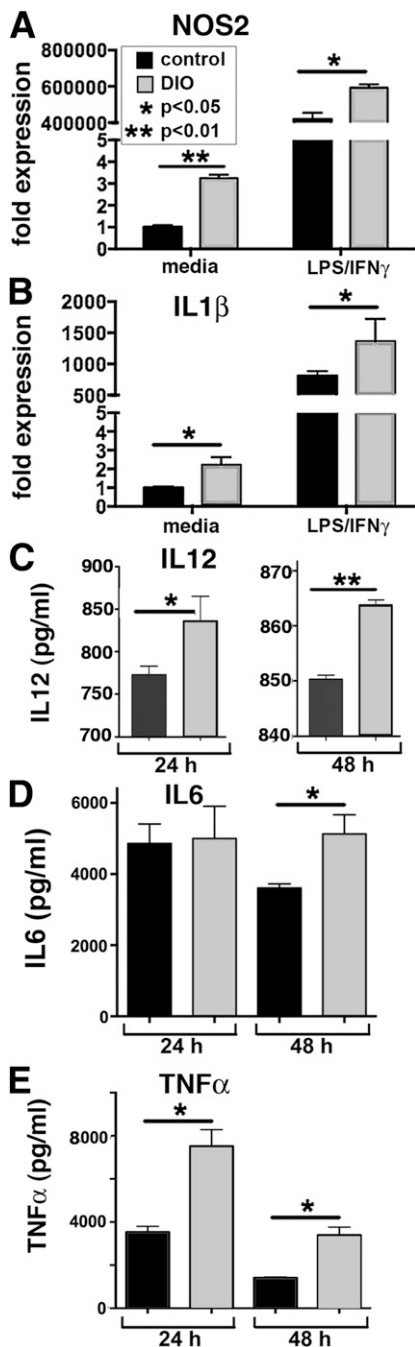
Figure 3—Macrophages are predisposed toward a proinflammatory (M1) phenotype in a T2D murine model. *A* and *B*: *NOS2* and *IL-1β* expression levels quantified by RT-PCR in DIO and control BMDMs at 6 and 24 h after stimulation with LPS/IFN-γ (*n* = 4, replicated two times). *C*: Levels of IL-12 in supernatants from DIO and control BMDMs following treatment with LPS/IFN-γ at 24 and 48 h as measured by ELISA (*n* = 4, plated in triplicate). *D* and *E*: Levels of IL-6 and TNF-α in supernatants from DIO and control BMDMs following treatment with LPS/IFN-γ at 24 and 48 h as measured by Bioplex. Protein levels are expressed as pg/mL (*n* = 4, plated in triplicate). Data are expressed as mean ± SE.

Figure 4—DIO BM stem/progenitor cells and peripheral macrophages display decreased trimethylation of H3K27me3 on the *IL-12* promoter. *A*: H3K27me3 levels in BM stem/progenitor cells (lin⁻/Sca1⁺/c-Kit⁺) and BMDMs (CD11b⁺/F4/80⁺) from DIO and control mice measured by flow cytometry (*n* = 4). *B–D*: BM stem/progenitor cells (lin⁻/c-Kit⁺), wound, and EWAT macrophages (CD11b⁺) were isolated in vivo using MACS and analyzed by ChIP for H3K27me3 levels on the promoter of *IL-12* (*n* = 3/group, plated in triplicate). *E*: H3K27me3 methylation was measured along the *IL-12* promoter in BMDMs (*n* = 3, replicated twice). Data are expressed as mean ± SE. MFI, mean fluorescence intensity; TSS, transcription start site.

macrophage polarization and that LPS-treated macrophages incubated with a Jmjd3 inhibitor demonstrated a reduction in proinflammatory cytokines, including IL-12 (20,21,27,29). A superarray was performed on CD11b⁺

MACS-isolated cells from peripheral wounds at day 3 postwounding, which demonstrated an over 23-fold increase in Jmjd3 in CD11b⁺ cells from DIO wounds compared with controls (Fig. 5A). Since H3K27me3 was decreased in the DIO CD11b⁺ wound cells and the BM LK cells, we investigated the relationship between Jmjd3 and H3K27me3 in the DIO BM. The amount of Jmjd3 transcript present in vivo in BM LK cells and BMDMs is significantly increased in the DIO cells compared with controls (Fig. 5B). Further, Jmjd3 levels are significantly increased in BM isolates from human T2D patients compared with nondiabetic controls (Fig. 5C). In addition, ChIP of H3K4me3 at the *Jmjd3* promoter in DIO LK cells
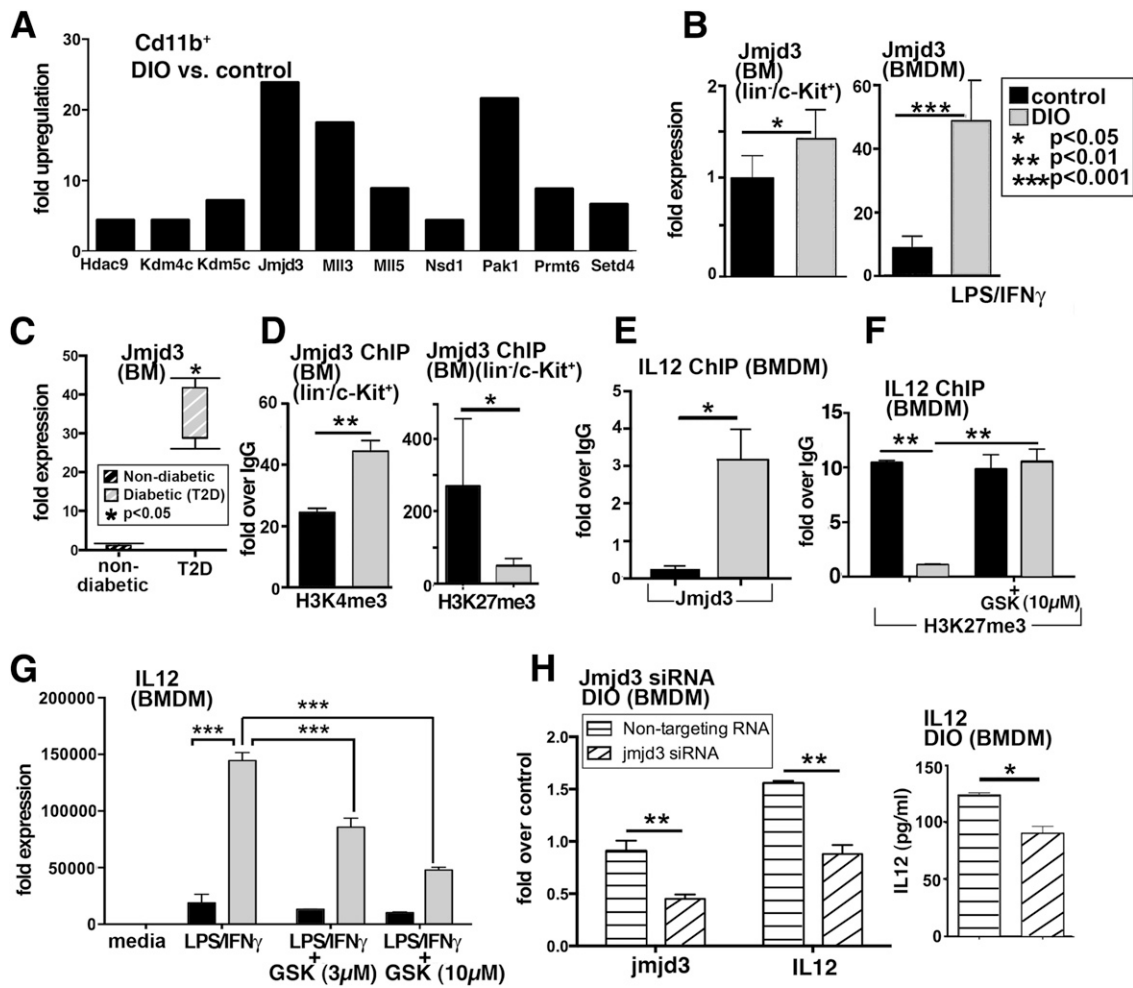
Figure 5—Increased JmjC demethylase, Jmjd3, production in BM LK cells and macrophages. *A*: Gene expression of chromatin-modifying enzymes was analyzed using PCR array plates in CD11b^{+} MACS-isolated cells from DIO and control wounds at day 3. Enzymes that were upregulated are shown. The threshold was set to a fourfold difference. Data are expressed as fold over control (*n* = 3/group). *B*: RT-PCR quantification of *Jmjd3* levels in DIO and control BM progenitor cells (lin[−]/c-Kit[+]) (isolated by MACS) and BMDMs (following stimulation with LPS/IFN-γ) (*n* = 4/group). *C*: RT-PCR analysis of human BM isolated from nondiabetic and T2D patients undergoing amputations at the femur level (*n* = 2/group). *D*: ChIP analysis of H3K4me3 and H3K27me3 on the *Jmjd3* promoter of in vivo MACS-isolated BM LK cells from DIO and control mice (*n* = 5/group). *E*: ChIP analysis for Jmjd3 on the *IL-12* promoter in DIO BMDMs compared with controls (*n* = 3/group, replicated once). *F*: BMDMs from DIO and control mice were treated with the H3K27me3 demethylase inhibitor, GSK-J4 (10 μmol/L), for 6 h, and ChIP analysis of H3K27me3 on the *IL-12* promoter was performed (*n* = 3/group). *G*: BMDMs from DIO and control mice were stimulated with LPS/IFN-γ in the presence or absence of GSK-J4 (3 μmol/L, 10 μmol/L) for 6 h, and analysis of *IL-12* transcription was performed (*n* = 3/group). Data are expressed as mean ± SE. *H*: DIO BMDMs were transfected with Jmjd3 siRNA or nontargeting siRNA or lipofectamine alone in triplicate wells. Forty-eight hours later, cells were stimulated with LPS/IFN-γ for 24 h. Transcript levels of *Jmjd3* and *IL-12* in cells treated with Jmjd3 siRNA or nontargeting siRNA are shown. Following stimulation, cell supernatants were collected and used for IL-12 Bioplex. Results are expressed as mean ± SE. Statistical analysis was performed using Student *t* tests, and *P* value <0.05 was considered significant.

demonstrated a significant increase in H3K4 trimethylation, resulting in an open chromatin conformation and increased gene expression. Further, a trend toward decreased gene repression (H3K27me3) was observed in the DIO LK cells at the *Jmjd3* promoter, allowing for increased Jmjd3 gene expression (Fig. 5D). A ChIP analysis of Jmjd3 levels on the *IL-12* promoter showed significantly increased Jmjd3 on the *IL-12* promoter in DIO macrophages as opposed to controls (Fig. 5E). To assess the biological relevance of Jmjd3-directed histone remodeling in the DIO BM cells and macrophages, we

used the newly generated H3K27 demethylase inhibitor, GSK-J4, the first selective inhibitor shown to prevent the Jmjd3-induced loss of H3K27me3 (20). In DIO BMDMs, GSK-J4 increased H3K27me3-mediated repression at the *IL-12* promoter, suggesting that modulation of Jmjd3 may alter the epigenetic signature at the *IL-12* promoter in the DIO setting (Fig. 5F). Importantly, when BMDMs were treated with LPS/IFN-γ, GSK-J4 decreased *IL-12* production in a dose-dependent fashion (Fig. 5G). Similar trends were observed in two other inflammatory cytokines (Supplementary Fig. 4A and B). In order to

more specifically examine the effects of Jmjd3, we targeted Jmjd3 using siRNA. Following specific reduction in Jmjd3 levels in DIO macrophages, we observed a significant reduction in *IL-12* in the DIO macrophages treated with Jmjd3-specific siRNA as compared with the DIO macrophages treated with a scrambled sequence (Fig. 5*H*). Thus, both the chemical inhibitor and specific Jmjd3-targeted siRNA were able to effectively reverse IL-12 expression in DIO macrophages.

BM Chimeras Demonstrate That the Peripheral Wound M1-Dominant Macrophage Phenotype Is Set at the BM Level

To evaluate whether the peripheral macrophage phenotype is controlled by BM stem/progenitor cells, BM chimeric mice were created. We created two groups of chimeric mice: *1*) GFP⁺DIO (mice on an HFD) BM donors into ND C57BL/6 recipients and *2*) GFP⁺ND BM donors into ND C57BL/6 recipients (30). Degree of chimerism was found to be 96.7% at 8 weeks posttransplant (Fig. 6*A*) using peripheral blood flow cytometry (31). Wound healing was significantly delayed in the WT mice receiving DIO BM (GFP⁺HFD BM donors into ND C57BL/6 recipients), compared with controls (Fig. 6*B*). Expression of *Jmjd3* and *IL-12* in CD11b⁺ wound macrophages was also increased in the chimeric mice receiving DIO BM, suggesting that H3K27 trimethylation in BM cells may play a key role in promoting the exaggerated proinflammatory response seen in diabetic macrophages (Fig. 6*C* and *D*).

DISCUSSION

The role of macrophages in chronic inflammation development associated with obesity and T2D has been well studied; however, how macrophages maintain a proinflammatory environment and promote chronic inflammation in T2D wounds has not been defined (32). In these studies, we used the DIO model to evaluate the origins of dysfunctional wound healing. The DIO mouse has progressive obesity, dyslipidemia, hyperglycemia, and poor wound healing, paralleling that seen in humans, and

does not have the potential for T-cell dysfunction seen in *db/db* mice and *ob/ob* mice due to deficient leptin signaling (28,33–35). Here, we demonstrate that macrophages in DIO wounds are poised, via an epigenetic mechanism, toward an unrestrained "M1-like" or proinflammatory activation state and produce significantly higher IL-12 levels. This prolongs the inflammatory phase and complicates the healing process by slowing resolution of wound site inflammation. The precise molecular and cellular mechanisms leading to alterations in the epigenetic signature remain to be determined but could reflect additional targets for directed therapy.

Our findings represent the first report on the role of epigenetics in BM cells and macrophages in obese, insulin-resistant T2D conditions and the resultant effects on modulating peripheral macrophage function/phenotype in wound healing. If monocytes mobilized to circulation from the BM are already poised toward a proinflammatory phenotype, then clinical treatments aimed at changing the local environment become less efficacious as they fail to address the systemic problem with the BM cells and macrophage polarization in T2D. Recent studies aimed at improving diabetic wound healing have focused on improving stem cell mobilization, which has resulted in only a modest improvement in angiogenesis and wound healing. These studies have failed to address the excessive number of inflammatory monocyte macrophages that perpetuate chronic inflammation in T2D wounds, and hence, T2D patients have not seen significant benefits from stem cell therapies directed at wound healing (36,37). Thus strategies aimed at altering these epigenetic changes at the BM level could significantly influence immune cell function in peripheral tissues and improve diabetic wound healing and potentially other secondary complications of T2D. Our findings provide a rationale for further studies targeting key epigenetic enzymes at the BM and local levels in order to promote an anti-inflammatory, repair macrophage phenotype and alter the inflammatory cascade maintained by unrestrained
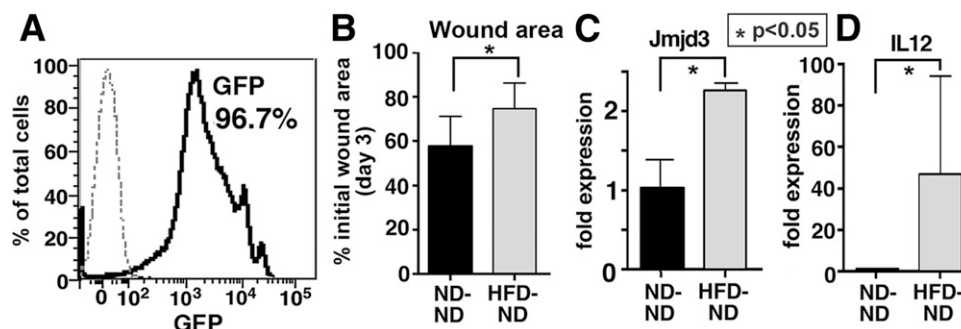
Figure 6—Wound healing is impaired and macrophage function is altered in GFP⁺DIO BM chimeras. BM chimeras were created using GFP⁺ mice on a C57BL/6 background. GFP⁺ mice were fed an HFD (60% fat) or ND (12% fat) for 14 weeks, and BM from these mice was transferred into irradiated C57BL/6 recipients. *A*: Peripheral blood analysis was performed weekly and at 8 weeks confirmed 96.5% donor chimerism. *B*: Change in wound area compared with initial wound size at day 3 postwounding (*n* = 4/group). *C* and *D*: *Jmjd3* and *IL-12* expression in in vivo macrophages (CD11b⁺) MACS isolated from wounds at day 3 were quantified by RT-PCR in ND→ND and HFD→ND GFP⁺ chimeric mice (*n* = 4/group). Data are expressed as mean ± SE.

proinflammatory activation in the setting of diabetic wounds. Hence, these data provide the foundation for significant improvements in existing clinical protocols for this significant unresolved epidemic.

Although the H3K27 demethylase Jmjd3 has been shown to influence polarization of macrophages in vitro, the role of this epigenetic enzyme in a pathological condition such as T2D is unknown (21). It stands to reason that the epigenetic signature differs during chronic inflammatory disease states. In this study, we found a potential new role for Jmjd3/KDM6B in modulating *IL-12* expression by macrophages in the setting of T2D. This is in agreement with a recent study where treatment of macrophages with a selective Jmjd3 inhibitor led to alterations in proinflammatory cytokines (20). As mentioned earlier, the DIO mouse may better reflect human physiology than some genetic models. However, it is not possible to determine the degree to which the observed changes in histone methylation are due to nutrient overconsumption and obesity, insulin resistance, or hyperglycemia. Further work is needed to investigate how changes in epigenetic signatures in metabolic diseases affect gene expression and how these chromatin modifications can be altered to achieve therapeutic benefit.

Since a large proportion of macrophages present at a wound site are recruited from the circulation and are not resident skin macrophages, we chose to focus on day 3 postwounding so that circulating monocytes had adequate time to enter the tissues, transform into macrophages, and perform a function (2,38). This is consistent with previous work that has demonstrated that at day 3 postwounding, recruited macrophage numbers are at their highest levels (39). Although controversy exists regarding the most accurate markers to define macrophage subsets, surface markers in isolation do not fully differentiate subpopulations of macrophages (40,41). Rather, the functional activity of macrophages plays an important role in defining potential macrophage subtypes (42,43). Among the many differences between activation of macrophages, the ratio of IL-12 to IL-10 appears important for distinguishing macrophage phenotypes (44). M1-like macrophages promote an inflammatory immune response through, among other cytokines, the production of IL-12. Thus, we focused on the production of IL-12 by macrophages as a defining characteristic of the proinflammatory (M1) macrophages (45). Although IL-10 and IL-12 are largely produced by macrophages, these cytokines can be affected by the local environment, including other immune cell types, including T lymphocytes and dendritic cells, that are present in smaller numbers following wounding (46).

Although we have examined how changes in the BM affect macrophage phenotype, other factors undoubtedly play a role in the complex process of wound healing. The function of macrophages during wound repair is likely influenced by both changes in cell programming and by the local microenvironment present at the wound site.

Several studies have supported a role for the local wound environment in regulating macrophage function (47). These studies found that blocking the proinflammatory cytokine IL-1β at the local level downregulates proinflammatory macrophages and promotes wound healing (48). From a clinical standpoint, in order to fully restore wound healing in T2D, therapies will need to promote an appropriate M1/M2 balance throughout the course of healing. Initially, proinflammatory macrophages are needed in the wound to clear debris and infection; however, conversion to an M2 anti-inflammatory response is needed in order for collagen deposition to occur at the appropriate time in the wound healing cascade (47). In this sense, therapies that target systemic changes in the BM stem cells, influence peripheral phenotypes, and restore a more "normal" macrophage balance are more attractive than just blocking the proinflammatory phenotype at the local wound site.

Macrophages are key orchestrators in the wound healing of many tissue types, including peripheral wounds. The prolonged presence of macrophages in wounds of both diabetic mice and human wounds suggests they are critical for restoring healing in T2D. Our group has recently examined macrophage polarization and found that macrophage phenotypes behave functionally similar in both murine models and humans (23). Macrophages from human venous ulcers have been shown to exhibit a similar proinflammatory phenotype to that observed in our human T2D wounds (49). The mechanism proposed for the M1 phenotype in the venous ulcers was due to excess iron, since hemosiderin deposits are clinically apparent in chronic venous ulcers. Thus, this is likely a specific pathway in the venous ulcer disease process, as diabetic wounds do not contain hemosiderin (49). In diabetic arterial wounds, other pathways are likely involved in promoting the proinflammatory macrophage phenotype.

In summary, we find that the insulin-resistant, hyperglycemic environment results in epigenetic changes in the bone marrow that persist in peripheral wounds. These changes, triggered in part by the signaling-independent activation of the transcription factor Jmjd3, result in the expression of inflammatory cytokines (IL-12) and lead to persistent wound inflammation. The identification of epigenetic changes in the BM stem/progenitor cells as an inciting event in the complex pathological process of inflammation has relevance to wound healing and may also play a role in persistent inflammation seen in other tissues in insulin resistance and T2D, such as adipose tissue and arterial walls (50,51). The T2D-related factors that trigger these epigenetic changes remain uncertain but understanding them may provide a path to preventing macrophage dysfunction and associated pathologies.

References

1. Driver VR, Fabbi M, Lavery LA, Gibbons G. The costs of diabetic foot: the economic case for the limb salvage team. J Vasc Surg 2010;52(Suppl.):17S–22S
2. Fathke C, Wilson L, Hutter J, et al. Contribution of bone marrow-derived cells to skin: collagen deposition and wound repair. Stem Cells 2004;22:812–822
3. Okuno Y, Nakamura-Ishizu A, Kishi K, Suda T, Kubota Y. Bone marrow-derived cells serve as proangiogenic macrophages but not endothelial cells in wound healing. Blood 2011;117:5264–5272
4. Sica A, Mantovani A. Macrophage plasticity and polarization: in vivo veritas. J Clin Invest 2012;122:787–795
5. Martin P. Wound healing—aiming for perfect skin regeneration. Science 1997;276:75–81
6. Benoit M, Desnues B, Mege JL. Macrophage polarization in bacterial infections. J Immunol 2008;181:3733–3739
7. Mantovani A, Sozzani S, Locati M, Allavena P, Sica A. Macrophage polarization: tumor-associated macrophages as a paradigm for polarized M2 mononuclear phagocytes. Trends Immunol 2002;23:549–555
8. Trinchieri G. Interleukin-12 and the regulation of innate resistance and adaptive immunity. Nat Rev Immunol 2003;3:133–146
9. Sutterwala FS, Noel GJ, Clynes R, Mosser DM. Selective suppression of interleukin-12 induction after macrophage receptor ligation. J Exp Med 1997; 185:1977–1985
10. Martinez FO, Sica A, Mantovani A, Locati M. Macrophage activation and polarization. Front Biosci 2008;13:453–461
11. Falanga V. Wound healing and its impairment in the diabetic foot. Lancet 2005;366:1736–1743
12. Porcheray F, Viaud S, Rimaniol AC, et al. Macrophage activation switching: an asset for the resolution of inflammation. Clin Exp Immunol 2005;142:481–489
13. Loots MA, Lamme EN, Zeegelaar J, Mekkes JR, Bos JD, Middelkoop E. Differences in cellular infiltrate and extracellular matrix of chronic diabetic and venous ulcers versus acute wounds. J Invest Dermatol 1998;111:850–857
14. Wetzler C, Kämpfer H, Stallmeyer B, Pfeilschifter J, Frank S. Large and sustained induction of chemokines during impaired wound healing in the genetically diabetic mouse: prolonged persistence of neutrophils and macrophages during the late phase of repair. J Invest Dermatol 2000;115:245–253
15. Hirahara K, Vahedi G, Ghoreschi K, et al. Helper T-cell differentiation and plasticity: insights from epigenetics. Immunology 2011;134:235–245
16. Jaenisch R, Bird A. Epigenetic regulation of gene expression: how the genome integrates intrinsic and environmental signals. Nat Genet 2003;33 (Suppl.):245–254
17. Schlesinger Y, Straussman R, Keshet I, et al. Polycomb-mediated methylation on Lys27 of histone H3 pre-marks genes for de novo methylation in cancer. Nat Genet 2007;39:232–236

18. Guenther MG, Levine SS, Boyer LA, Jaenisch R, Young RA. A chromatin landmark and transcription initiation at most promoters in human cells. Cell 2007; 130:77–88
19. Krausgruber T, Blazek K, Smallie T, et al. IRF5 promotes inflammatory macrophage polarization and TH1-TH17 responses. Nat Immunol 2011;12: 231–238
20. Kruidenier L, Chung CW, Cheng Z, et al. A selective jumonji H3K27 demethylase inhibitor modulates the proinflammatory macrophage response. Nature 2012;488:404–408
21. Ishii M, Wen H, Corsa CA, et al. Epigenetic regulation of the alternatively activated macrophage phenotype. Blood 2009;114:3244–3254
22. Wen H, Dou Y, Hogaboam CM, Kunkel SL. Epigenetic regulation of dendritic cell-derived interleukin-12 facilitates immunosuppression after a severe innate immune response. Blood 2008;111:1797–1804
23. Kittan NA, Allen RM, Dhaliwal A, et al. Cytokine induced phenotypic and epigenetic signatures are key to establishing specific macrophage phenotypes. PLoS ONE 2013;8:e78045
24. Martinez FO, Gordon S, Locati M, Mantovani A. Transcriptional profiling of the human monocyte-to-macrophage differentiation and polarization: new molecules and patterns of gene expression. J Immunol 2006;177:7303–7311
25. Gallagher KA, Liu ZJ, Xiao M, et al. Diabetic impairments in NO-mediated endothelial progenitor cell mobilization and homing are reversed by hyperoxia and SDF-1 alpha. J Clin Invest 2007;117:1249–1259
26. Shaul ME, Bennett G, Strissel KJ, Greenberg AS, Obin MS. Dynamic, M2-like remodeling phenotypes of CD11c+ adipose tissue macrophages during high-fat diet—induced obesity in mice. Diabetes 2010;59:1171–1181
27. De Santa F, Totaro MG, Prosperini E, Notarbartolo S, Testa G, Natoli G. The histone H3 lysine-27 demethylase Jmjd3 links inflammation to inhibition of polycomb-mediated gene silencing. Cell 2007;130:1083–1094
28. Lam QL, Lu L. Role of leptin in immunity. Cell Mol Immunol 2007;4:1–13
29. Satoh T, Takeuchi O, Vandenbon A, et al. The Jmjd3-Irf4 axis regulates M2 macrophage polarization and host responses against helminth infection. Nat Immunol 2010;11:936–944
30. Dolgachev VA, Ullenbruch MR, Lukacs NW, Phan SH. Role of stem cell factor and bone marrow-derived fibroblasts in airway remodeling. Am J Pathol 2009; 174:390–400
31. Morrison SJ, Wandycz AM, Hemmati HD, Wright DE, Weissman IL. Identification of a lineage of multipotent hematopoietic progenitors. Development 1997;124:1929–1939
32. Weisberg SP, McCann D, Desai M, Rosenbaum M, Leibel RL, Ferrante AW Jr. Obesity is associated with macrophage accumulation in adipose tissue. J Clin Invest 2003;112:1796–1808
33. Dixit VD, Schaffer EM, Pyle RS, et al. Ghrelin inhibits leptin- and activation-induced proinflammatory cytokine expression by human monocytes and T cells. J Clin Invest 2004;114:57–66
34. De Rosa V, Procaccini C, Calì G, et al. A key role of leptin in the control of regulatory T cell proliferation. Immunity 2007;26:241–255
35. Parekh PI, Petro AE, Tiller JM, Feinglos MN, Surwit RS. Reversal of diet-induced obesity and diabetes in C57BL/6J mice. Metabolism 1998;47:1089–1096
36. Tateishi-Yuyama E, Matsubara H, Murohara T, et al.; Therapeutic Angiogenesis using Cell Transplantation (TACT) Study Investigators. Therapeutic angiogenesis for patients with limb ischaemia by autologous transplantation of bone-marrow cells: a pilot study and a randomised controlled trial. Lancet 2002;360:427–435
37. Walter DH, Krankenberg H, Balzer JO, et al.; PROVASA Investigators. Intra-arterial administration of bone marrow mononuclear cells in patients with critical limb ischemia: a randomized-start, placebo-controlled pilot trial (PROVASA). Circ Cardiovasc Interv 2011;4:26–37
38. Wu Y, Wang J, Scott PG, Tredget EE. Bone marrow-derived stem cells in wound healing: a review. Wound Repair Regen 2007;15(Suppl. 1):S18–S26
39. Leibovich SJ, Ross R. The role of the macrophage in wound repair. A study with hydrocortisone and antimacrophage serum. Am J Pathol 1975;78: 71–100

40. Vogel DY, Vereyken EJ, Glim JE, et al. Macrophages in inflammatory multiple sclerosis lesions have an intermediate activation status. J Neuro-inflammation 2013;10:35

41. Martinez FO, Helming L, Milde R, et al. Genetic programs expressed in resting and IL-4 alternatively activated mouse and human macrophages: similarities and differences. Blood 2013;121:e57–e69

42. Biswas SK, Mantovani A. Macrophage plasticity and interaction with lymphocyte subsets: cancer as a paradigm. Nat Immunol 2010;11:889–896

43. Geissmann F, Manz MG, Jung S, Sieweke MH, Merad M, Ley K. Development of monocytes, macrophages, and dendritic cells. Science 2010;327:656–661

44. Duluc D, Delneste Y, Tan F, et al. Tumor-associated leukemia inhibitory factor and IL-6 skew monocyte differentiation into tumor-associated macrophage-like cells. Blood 2007;110:4319–4330

45. Stout RD, Jiang C, Matta B, Tietzel I, Watkins SK, Suttles J. Macrophages sequentially change their functional phenotype in response to changes in microenvironmental influences. J Immunol 2005;175:342–349

46. Toulon A, Breton L, Taylor KR, et al. A role for human skin-resident T cells in wound healing. J Exp Med 2009;206:743–750

47. Barrientos S, Stojadinovic O, Golinko MS, Brem H, Tomic-Canic M. Growth factors and cytokines in wound healing. Wound Repair Regen 2008;16:585–601

48. Mirza RE, Fang MM, Ennis WJ, Koh TJ. Blocking interleukin-1β induces a healing-associated wound macrophage phenotype and improves healing in type 2 diabetes. Diabetes 2013;62:2579–2587

49. Sindrilaru A, Peters T, Wieschalka S, et al. An unrestrained proinflammatory M1 macrophage population induced by iron impairs wound healing in humans and mice. J Clin Invest 2011;121:985–997

50. Lumeng CN, Deyoung SM, Bodzin JL, Saltiel AR. Increased inflammatory properties of adipose tissue macrophages recruited during diet-induced obesity. Diabetes 2007;56:16–23

51. Parathath S, Grauer L, Huang LS, et al. Diabetes adversely affects macrophages during atherosclerotic plaque regression in mice. Diabetes 2011;60:1759–1769